Article

Verification of Biochemical Activity for Proteins Nanografted on Gold Surfaces

Cristian Staii, David W. Wood, and Giacinto Scoles

J. Am. Chem. Soc., **2008**, 130 (2), 640-646 • DOI: 10.1021/ja076157+

J|A|C|S
ARTICLES
Published on Web 12/15/2007

Verification of Biochemical Activity for Proteins Nanografted on Gold Surfaces

Cristian Staii,*[,†,||] David W. Wood,[‡] and Giacinto Scoles[†,§]

Departments of Chemistry, Chemical Engineering, and Molecular Biology, Princeton University, Princeton, New Jersey 08544, and SISSA-ELLETRA Nano Innovation Laboratory, ELETTRA Sincrotrone Trieste Strada Statale 14, 34012 Basovizza, Trieste, Italy

Received August 15, 2007; E-mail: cstaii@princeton.edu

Abstract: We demonstrate that the Atomic Force Microscope (AFM) can be used to immobilize a dicysteine-terminated protein (Maltose Binding Protein, MBP-cys-cys for short) at well-defined locations directly on gold substrates via nanografting and characterize the in situ bioactivity of these proteins within the fabricated nanopatterns. This method exploits the high spatial and orientational control of the protein monolayer assembly allowed by nanografting, combined with the high sensitivity of the AFM for detecting ligand-binding events. The maltose-mediated conformational changes within the MBP have been found to change the AFM−tip−protein interaction, therefore causing the frictional signal to change. Our measurements show that the protein ligand-binding function is maintained upon the immobilization process and is not affected by (a) the addition of the cysteine dipeptide, (b) the spatial confinement associated with nanografting, and (c) the interaction between the protein and the Au substrate. These surface-confined proteins can also be regenerated, and their frictional response is reproducible through several maltose exposure/washing cycles. By measuring the change in the frictional force above the protein nanopatterns as a function of maltose concentration, we determined the dissociation constant for the MBP-cys-cys/maltose system to be kd = (1 ± 0.04) μM. Our results show that the MBP-cys-cys system provides a very sensitive surface-based, protein nanobiosensor for maltose detection at the attogram level (∼100 nM concentration). The implications of our study for the fabrication of molecular-scale biological sensors are discussed at the end of the paper.

1. Introduction

The interface of nanoengineering with biology and medicine is an emerging frontier with the potential for offering numerous therapeutic, diagnostic, and analytical solutions. In particular, both natural and artificially designed proteins with high affinity and excellent selectivity for specified target molecules (analytes) have great potential for applications in nanoscale biosensors. The ability of proteins to specifically bind other target proteins or ligands underlies innumerable life processes and medical treatments that range from cell−cell communication to hormonal activity and to the targeted delivery of chemotherapeutic agents to cancer cells.[1,2]

One very promising approach to protein-based biosensor design is to couple this extraordinary molecular recognition capability to an appropriate detection device, such as an electronically addressable substrate upon which the proteins can be mounted.[3] This leads to the fabrication of protein microarrays, which consist of libraries of proteins immobilized in a two-dimensional addressable grid on a chip. However, one of the major issues for this technology lies in the successful development of robust strategies to allow efficient immobilization of proteins onto atomically planar surfaces while maintaining their native biological functions.[2,4,5]

Biomolecule patterning on the scale of a few hundreds of nanometers can now readily be accomplished using common microfabrication techniques such as photolithography,[6−8] ion beam and electron beam lithography,[9−12] use of multicomponent organic thin films,[13] microfluidic networks,[14,15] and microcontact

† Department of Chemistry, Princeton University.
‡ Departments of Chemical Engineering and Molecular Biology, Princeton University.
§ SISSA-ELLETRA Nano Innovation Laboratory.
|| Current address: Department of Physics, University of Wisconsin, Madison, 1150 University Avenue, Madison, WI 53706.

(1) Medintz, I. L.; Deschamps, J. R. *Curr. Opin. Biotechnol.* **2006**, *17*, 17−27.
(2) Phizicky, E.; Bastiaens, P. I. H.; Snyder, M.; Fields, S. *Nature* **2003**, *422*, 208−215.
(3) Collings, A. F.; Caruso, F. *Rep. Prog. Phys.* **1997**, *60*, 1397−1445.
(4) Talapatra, A.; Rouse, R.; Hardiman, G. *Pharmacogenomics* **2002**, *3*, 1−10.
(5) Girish, A.; Sun, H.; Yeo, D. S. Y.; Chen, G. Y. J.; Chua, T. K.; Yao, S. Q. *Bioorg. Med. Chem. Lett.* **2005**, *15*, 2447−2451.
(6) Hengsakul, M.; Cass. A. E. G. *Bioconjugate Chem.* **1996**, *7*, 249−254.
(7) Liu, J.; Hlady, V. *Colloids Surf., B* **1996**, *8*, 25−37.
(8) Bernard, A.; Delamarche, E.; Schmid, H.; Michel, B.; Bosshard, H. R.; Biebuyck, H. *Langmuir* **1998**, *14*, 225−229.
(9) Bergman, A. A.; Buijs, J.; Herbig, J.; Mathes, D. T.; Demarest, J. J.; Wilson, C. D.; Reimann, C. T.; Baragiola, R. A.; Hull, R.; Oscarsson, S. O. *Langmuir* **1998**, *14*, 6785- 6788.
(10) Tiberio, R. C.; Craighead, H. G.; Lercel, M.; Lau, T.; Sheen, C. W.; Allara, D. L. *Appl. Phys. Lett.* **1993**, *62*, 476−478.
(11) Sondag-Huethorst, J. A. M.; VanHelleputte, H. R. J.; Fokkink L. G. J. *Appl. Phys. Lett.* **1994**, *64*, 285−287.
(12) Harnett, C. K.; Satyalakshmi, M.; Craighead, H. G. *Langmuir* **2001**, *17*, 178−182.
(13) Fang, J.; Knobler, C. M. *Langmuir* **1996**, *12*, 1368−1374.
(14) Patel, N.; Sanders, G. H. W.; Shakesheff, K. M.; Cannizzaro, S. M.; Davies, M. C.; Langer, R.; Roberts, C. J.; Tendler, S. J. B.; Williams, P. M. *Langmuir* **1999**, *15*, 7252−7257.
(15) Kim, Y.-D.; Park, C. B.; Clark, D. S. *Biotechnol. Bioeng.* **2001**, *73*, 331−337.

 10.1021/ja076157+ CCC: $40.75

printing.[16−18] The main challenges faced by any approach of the type mentioned above are the precise positioning of biomolecules on the substrate for the fabrication of small (<100 nm) patterns and the preservation of the configuration and bioactivity of the target through the multistep microfabrication process.

More recently, it has been shown that protein nanopatterns with precise control over pattern position, size, and geometry can be fabricated using an Atomic Force Microscope (AFM)-based lithography technique called nanografting.[19−22] This technique was first introduced as a very powerful tool to fabricate highly ordered, closed-packed nanopatterns of self-assembled monolayers of organic thiol-terminated molecules on gold substrates.[23,24] In nanografting, an AFM tip is used at a relatively high force to catalyze the exchange of the molecules of a self-assembled thiol monolayer (SAM), with other thiols of interest (organic molecules, proteins, DNA, etc.) present in an adjacent solution. This solution has the double function of diluting the molecules of the original SAM displaced by the tip and providing a reservoir for the replacing molecules. The nanostructures obtained can then be visualized *in situ* at low applied force values via topography measurements with the same AFM tip. For example, nanografting was used to produce patches of de novo S-824 protein amidst a surrounding monolayer of alkane thiols.[22] Nanografting offers several advantages for this type of work: (a) the procedure can be carried out in aqueous solutions (protein buffers containing a small amount of alcohol to facilitate the solubility of the displaced molecules); in this way the proteins are very likely to retain their folding conformation and therefore their bioactivity; (b) it allows the investigation of a conveniently small (nanoscale) region with well-defined boundaries; (c) measurement of molecular heights above the substrate can be done with very good precision (of the order of 1 Å), which allows identification of the molecular orientation of the protein; (d) in principle it allows patterning of multifunctional devices by the sequential adsorption of a series of proteins with different functionalities at different addressable locations on the same chip; (e) finally, nanografted patches are, in general, better ordered than the surrounding SAM, and therefore these patches are resistant to the force exerted by the AFM tip; this characteristic enables probing of the structural stability of proteins packed at high densities.[22]

In previous work, G.-Y. Liu and co-workers have successfully immobilized proteins on prepatterned SAMs using a two-step approach: (1) the production of nanometer-size patterns of SAMs on a surface using nanografting followed by (2) the selective adsorption of proteins onto these patterns via either electrostatic or covalent interactions.[19,20] In addition to the very high spatial resolution achieved (10 nm × 150 nm lines containing proteins) these experiments have also shown that the (indirectly attached) proteins within these nanostructures retain the ability to bind corresponding specific antibodies, and therefore their bioreactivity is preserved. Previous work done in our group has also applied nanografting to immobilize novel proteins at addressable locations on gold surfaces.[21,22] The attachment of proteins within our approach is carried out, however, *directly* on the Au surface and has the advantage of precisely controlling the orientation of the proteins, therefore allowing the use of AFM-measured height and (as it will be shown) friction to study/identify binding events.

The next step necessary for designing protein based nanosensors is to show that nanografting does not hinder their biological activity. In this paper we demonstrate that an AFM can be used to both *immobilize* proteins at well-defined locations *directly* on Au substrates via nanografting and *to characterize in situ the biological function* of the proteins within the fabricated nanopatterns. We also show that, in a well-ordered protein patch, AFM friction can be used to identify protein−ligand binding events.

Another important challenge presented by the process of protein microarray fabrication is the requirement for high-throughput expression and purification of proteins, because thousands of purified proteins are required for the generation of high-density protein microarrays.[1,2] Fortunately, over the past decade several technologies have been developed where target proteins are manipulated at the genetic level to increase productivity and simplify their purification. For example, the use of genetically fused affinity tags has become very common in research for purifying large numbers of proteins.[25] A recently developed method for high-throughput protein purification uses self-cleaving elastin-like polypeptides (ELP) fusion tags.[26−28] These tags consist of repeating pentapeptides (VPGXG with X being any amino acid except proline) fused to a controllable self-cleaving intein,[29] which is also attached to the target protein.[26] In this method, the ELP tag precipitates in response to small increases in temperature, allowing the fused target to be purified. Once this is completed, the target is released from the ELP-intein tag by the self-cleaving intein, and the tag is precipitated by gentle warming and then removed. A very important advantage of the ELP-intein purification method is that it allows purification of active protein directly from cell lysate in a single process and eliminates the need for expensive chromatography or affinity resins. The combination of low cost/high yield makes this approach not only an exciting new purification technology for future research but also a very powerful tool for manufacturing applications, such as protein based biosensors.[27]

Of particular importance for prototyping various biosensing platforms are the numerous proteins from the bacterial Periplasmic Binding Proteins (PBPs) family, such as: Maltose Binding Protein (MBP), Glucose Binding Protein (GBP), Ribose Binding Protein (RBP), etc.[1] The interest in utilizing this large

(16) Bieri, C.; Ernst, O. P.; Heyse, S.; Hofmann, K. P.; Vogel, H. *Nature* **1999**, *17*, 1105−1108.
(17) Bernard, A.; Renault, J. P.; Michel, B.; Bosshard, H. R.; Delamarche, E. *Adv. Mater.* **2000**, *12*, 1067−1070.
(18) Ta, T. C.; McDermott, M. T. *Anal. Chem.* **2000**, *72*, 2627−2634.
(19) Wadu-Mesthrige, K.; Amro, N. A.; Garno, J. C.; Xu, S.; Liu, G.-Y. *Biophys. J.* **2001**, *80*, 1891−1899.
(20) Liu, G-Y.; Amro, N. A. *Proc. Natl. Acad. Sci. U.S.A.* **2002**, *99*, 5165−5170.
(21) Case, M. A.; McLendon, G.; Hu, Y.; Vanderlick, T.; Scoles, G. *Nano Lett.* **2003**, *3*, 425−429.
(22) Hu, Y.; Das, A.; Hecht, M. H.; Scoles, G. *Langmuir* **2005**, *21*, 9103−9109.
(23) Xu, S.; Liu, G. Y. *Langmuir* **1997**, *13*, 127−129.
(24) Liu, G. Y.; Xu, S.; Qian, Y. *Acc. Chem. Res.* **2000**, *33*, 457−466.
(25) Terpe, K. *Appl. Microbiol. Biotechnol.* **2003**, *60*, 523−533.
(26) Banki, M. R.; Feng, L.; Wood D.W. *Nature Methods* **2005**, *2*, 659−662.
(27) Banki, M. R.; Wood, D. W. *Microb. Cell. Fact.* **2005**, *4*, 32.
(28) Ge, X.; Yang, D. S. C.; Trabbic-Carlson, K.; Kim, B.; Chilkoti, A.; Filipe, C. D. M. *J. Am. Chem. Soc.* **2005**, *127*, 11228−11229.
(29) Inteins (INTervening protEINs) are protein insertion sequences embedded in a larger host protein. A self-splicing intein both catalyzes its own removal from the host protein and ligates the flanking segments. The "self-splicing" process results in two separate product proteins (see refs 25, 30, and 31).

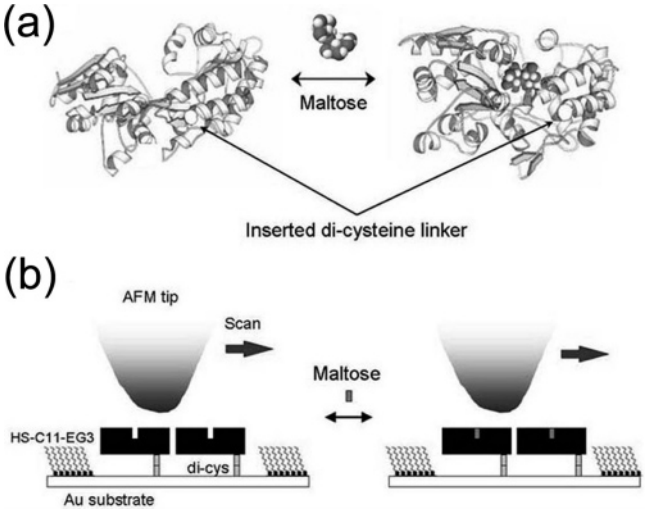

Figure 1. (a) Maltose-induced conformational change in Maltose Binding Protein. The structure of MBP is shown as a ribbon cartoon, generated using the protein data bank. Maltose is shown in a space-filling model. The COOH terminus of MBP, used as an attachment site for the double cysteine linker, is indicated by the arrows. MBP undergoes a conformational change ("hinge-bending motion") upon introducing maltose, from an "open" (ligand-free) state (*left*) to a "closed" (ligand-bound) state (*right*). (b) Schematic of MBP with a double-cysteine terminal linker nanografted into a undecanethiol triethylene glycol SAM on a Au substrate. The maltose induced "hinge bending motion" can be detected by AFM friction measurements (see text).

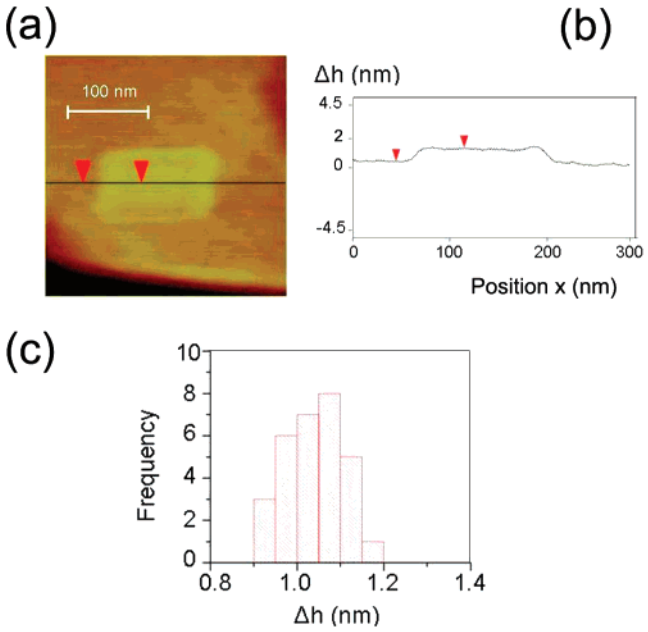

Figure 2. (a) AFM height image of a MBP-cys-cys protein patch nanografted into a HSC_{11}-EG_3 layer on a gold island. (b) Line scan corresponding to the black line in the height image (a). The measured height difference between the protein and the SAM in this case is 1 nm. (c) Histogram of the height differences between MBP-cys-cys and HSC_{11}-EG_3 layer, for 30 different protein patches of the kind shown in (a). The histogram peak is 1.06 nm which corresponds to an average protein height of 3.36 nm.

protein family for biosensing stems both from their very specific recognition of an extremely large class of analytes (ligands) in nanomolar concentrations (including various sugars, amino acids, phosphates, sulfates, metal ions, etc.)[1] and from their reversible ligand-dependent conformational change, which involves switching from an "open" (ligand-free) to a "closed" (ligand-bound) form (Figure 1). This unique conformational change is displayed by almost all PBPs and is based on their fundamental two-domain structural motif: two large polypeptide lobes, connected via flexible tethers ("hinge region"), which surround a central ligand-binding site. Ligand binding thus induces a large conformational change such that the two lobes bend and fold together (Figure 1a).

The aim of most PBP-based sensors is to detect this very specific recognition event with a biosensing signal transduction mechanism such as direct fluorescence,[1,32,33] electrochemical detection,[34] electron-transfer mediated fluorescence,[35,36] surface plasmon resonance,[37] and fluorescence resonance energy transfer (FRET).[38] For example, Benson and co-workers[34] have reported a flexible strategy for transducing ligand-binding events into electrochemical responses for a large variety of proteins from the PBP family, including MBP. In these studies the proteins were attached to the electrode by modifying the gold surface with a self-assembled monolayer of hydroxyl- and Ni(II)-nitrilotriacetate terminated headgroups and site-specifically linking the C-terminal oligohistidine-tagged protein. Although this method provides a consistent orientation of each protein, their locations are spatially random. To couple ligand binding to an electrochemical response, a thiol reactive Ru(II) complex was covalently linked to a mutant cysteine on the protein and used as a redox reporter group.

Electrochemistry is suitable for many protein-based sensor applications, but since the signal scales down with decreasing electrode area, there is a tradeoff between size and sensitivity that precludes detection of very low quantities of molecules down to or below the nanomolar level. On the other hand, AFM-based detection does not suffer from the same limitations. Indeed, if the AFM could be used for both fabrication and detection, this would increase the practicality of using this instrument for fabricating high sensitivity biosensors. For example, in the case of DNA molecules, G.Y. Liu and co-workers have used differential height measurements to detect hybridization of nanostructures consisting of no more than 10 000 DNA molecules each immobilized on Au surfaces.[39,40]

In the present work we report the nanografting and AFM characterization of Maltose Binding Protein (MBP), a structurally well-characterized member of the Periplasmic-Binding Protein (PBP) family.[1,34,38] We demonstrate that the AFM can be used both to immobilize cysteine terminated MBP at specific locations on a Au chip and to detect ligand (maltose) binding

(30) Perler, F. B.; Davis, E. O.; Dean, G. E.; Gimble, F. S.; Jack, W. E. *Nucleic Acids Res.* **1994**, *22*, 1125−1127.
(31) Liu, X.-Q. *Annu. Rev. Genet.* **2000**, *34*, 61−76.
(32) De Lorimier, R. M.; Smith, J. J.; Dwyer, M. A.; Looger, L. L.; Sali, K. M.; Paavola, C. D.; Rizk, S. S.; Sadigov, S.; Conrad, D. W.; Loew, L.; Hellinga, H. W. *Protein Sci.* **2002**, *11*, 2655−2675.
(33) Gilardi, G.; Zhou, L. Q.; Hibbert, L.; Cass, A. E. G. *Anal. Chem.* **1994**, *66*, 3840−3847.
(34) Benson, D. E.; Conrad, D. W.; Trammell, S.; Hellinga, H. W. *Science* **2001**, *293*, 1641−1644.
(35) Sandros, M. G.; Vivekanand, S.; Benson, D. E. *Analyst* **2006**, *131*, 229−235.
(36) Sandros, M. G.; Gao, D.; Benson, D. E. *J. Am. Chem. Soc.* **2005**, *127*, 12198−12199.
(37) Hsieh, H. V.; Pfeiffer, Z. A.; Amiss, T. J.; Sherman, D. B.; Pitner, J. B. *Biosens. Bioelectron.* **2004**, *19*, 653−660.
(38) Medintz, I. L.; Clapp, A. R.; Mattoussi, H.; Goldman, E. R.; Fisher, B.; Mauro, J. M. *Nat. Mater.* **2003**, *2*, 630−638.
(39) Liu, M.; Amro, N. A.; Chow, C. S.; Liu, G.-Y. *Nano Lett.* **2002**, *2*, 863−867.
(40) Liu, M.; Liu, G.-Y. *Langmuir* **2005**, *21*, 1972−1978.

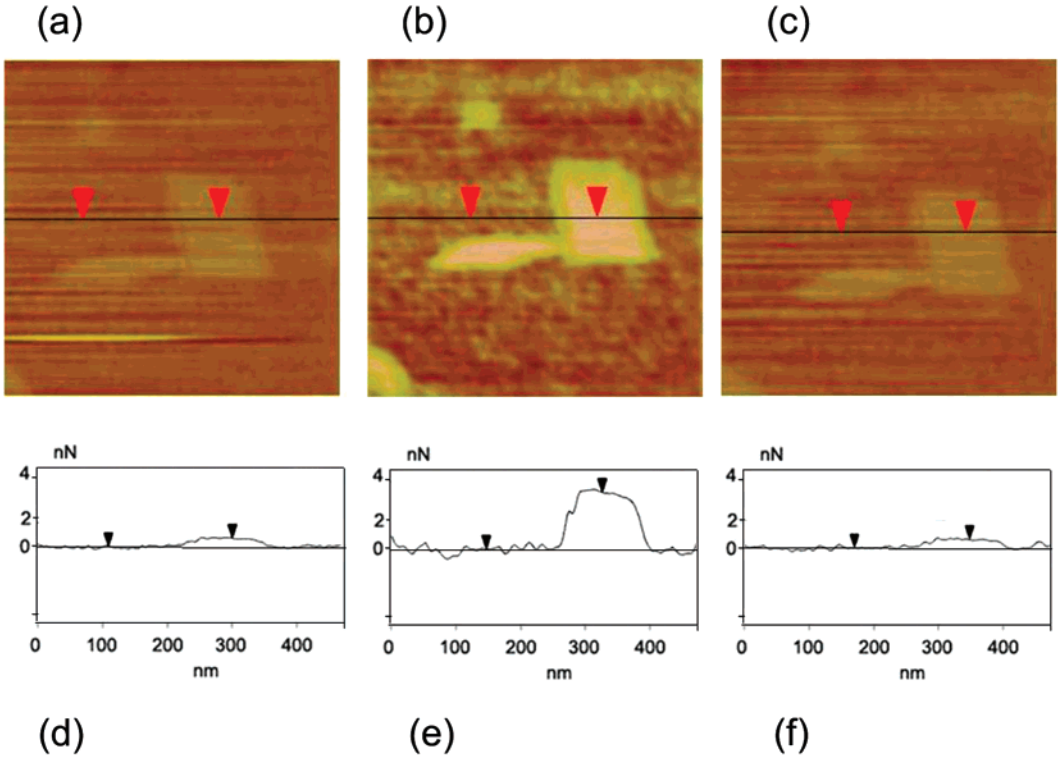

Figure 3. Lateral frictional force images of an area containing 2 MBP patches: (a) before adding maltose to the buffer solution, (b) after introducing maltose (0.2 μM), and (c) after removing the maltose solution and washing with protein buffer for 15 min. (d−f) Line scans corresponding to the black lines in image panels (a−c), respectively. Frictional data were recorded as photodiode output in millivolts. The conversion to lateral frictional force is done using the procedure outlined in ref 41. A clear increase in the frictional force above the protein patch is observed upon adding maltose to the system, as shown in images (b) and (e). The process is reversible, and the original value of the frictional force is recovered after washing the sample with protein buffer: (c), (f).

to MBP. We also show that the protein function is not altered by the addition of cysteins at its C terminus or the nanografting process. Furthermore, by measuring the variation of the frictional force between the AFM tip and the surface-immobilized protein molecules in response to changes in maltose concentration, we extract valuable information about the protein conformational changes and maltose binding kinetics. These results represent a further step forward toward fabricating and using protein-based biosensor arrays employing an AFM.

2. Experimental Methods

2.1. Protein Expression and Purification. Enzymes used for DNA modification, cloning, and analysis were purchased from New England Biolabs (Ipswich, MA). Standard recombinant DNA techniques were used in the construction of all vectors. The *E. coli* maltose-binding domain (MBD) was PCR-amplified from the New England Biolabs pMAL vector, where the 3′ PCR primer was designed to add two additional cysteine residues to the C-terminus of the expressed MBD. The fragment was then inserted into a previously reported ELP-intein purification vector,[26] using BsrG I and Hind III restriction sites. Expression and purification of the dicysteine terminated MBD was carried out as per the previously described method for the ELP-intein purification vector.[26] Based on previous work in our laboratories,[27] MBP-cys-cys yields were expected to be approximately 80 mg/L. During the nanografting experiments the MBP-cys-cys protein was solubilized (at concentrations 40−200 mg/L or 1−5 mM) in pH 6.5 buffer solution (1X PBS, 40 mM Bis-Tris, pH 6.5 with 2 mM EDTA and 1 mM DTT). DTT (1,4-dithiothreitol) was added to maintain the cysteine in the reduced state such that the protein is predominantly monomeric.[22] To enhance the solubility of the displaced alkanethiols during nanografting, 5% v/v trifluoroethanol (TFE) was added to the aqueous buffer.[21]

2.2. Substrate and SAM Preparation. The Au (111) surface was prepared by thermal evaporation on a mica substrate in a vacuum chamber (K. J. Lesker Co., EJ1800 Bell Jar) at a background pressure of 1×10^{-7} mbar. The mica (Ruby Muscovite mica, S & J Trading) was heated up to 300 °C for 5 h prior to evaporation. The temperature was kept constant at 300 °C during the evaporation. Typically, 1000 Å of gold (CERAC, 99.999% purity) were deposited on freshly cleaved mica at the rate of 0.2−0.3 Å/s. After metallization, the Au-coated mica was allowed to cool down to room temperature and the sample was taken out and immersed into a 0.1 mM undecanethiol triethylene glycol (Prochimia, 98% purity) solution. A compact monolayer was allowed to form on the Au(111) surface for 24 h. Before it was characterized by an AFM, the sample was rinsed for 5 min with pure ethanol (AAPER Alcohol and Chemical Co.) and dried by a gentle flow of nitrogen.

2.3. Nanografting, AFM Imaging, and Friction Measurements. Nanografting and imaging were both carried out using a Digital Instruments MultiMode AFM (Santa Barbara, CA) with a Nanoscope IIIa controller. The scanner (Type E, Digital Instruments) was calibrated in the *Z* direction by measuring atomically resolved gold steps. All experiments were carried out in a liquid cell kept at room temperature and placed in an acoustic isolation box (Molecular Imaging). Experiments were performed with commercially available V-shaped cantilevers with oxide-sharpened Si_3N_4 tips (NPS, Veeco Instruments) with a spring constant of 0.58 N/m. The cantilever dimensions reported by the manufacturer are 196 μm (length), 41 μm (width), and 0.6 μm (thickness). The cantilever's Young's modulus is 150 GPa, and the tip height is 3 μm. The process of nanografting has been described extensively elsewhere.[23,24] Basically, it consists of a three-step procedure: (a) an AFM tip is used, at low force, to image the surface morphology and select a flat region, typically 500 nm × 500 nm; (b) a portion of the selected area (typically 150 nm × 150 nm) is then

scanned at a higher load, to force the original SAM thiols to exchange with the cysteine terminated proteins from the buffer solution to form a "protein patch"; (c) finally, the nanografted protein patch is imaged at low force, and the orientation (height) of the proteins with respect to the original SAM is determined. For the friction measurements height and lateral force images in both trace and retrace directions were captured in contact mode for each protein patch. The trace and retrace images were subtracted and then divided by two and were converted into friction data utilizing the procedure outlined by Sader[41] with the cantilever parameters listed above. The concentration of MBP in the buffer solution was kept constant at 1 mM throughout all the experiments, whereas the maltose concentration was varied from 0 to 1 mM.

3. Results and Discussion

3.1. Nanografting MBP into PEG Layers. Since native MBP contains no cysteine residues, we have genetically engineered MBP to contain a double cysteine (cys-cys) linker at its C terminus (see Experimental Methods). The chemical link between the end-cysteine of the MBP and Au serves a double role: it provides a unique site for protein immobilization, and it also ensures that the MBP-cys-cys molecule has only one possible orientation on the Au substrate upon nanografting (the nanografting replaces the sulfur−gold interaction of the surrounding alkanethiol SAM with a sulfur−gold interaction involving the C-terminal cysteine of the protein). This arrangement is also designed to orient the maltose binding site toward the buffer solution (Figure 1).

Of the materials that have been identified as being able to form protein resistant SAMs, long chain poly(ethylene glycol) (PEG) polymers have attracted the most attention. Their protein-resistant properties have generally been explained with the following mechanism: when the protein diffuses into the interphase and compresses the PEG layer, an inhibition of protein adsorption may arise due to both an enthalpic penalty due to the desolvation of the PEG chains and a conformational entropy loss of the polymer chains.[42] Self-assembled monolayers of thiols, terminated with short oligomers of the ethylene glycol group ($[OCH_2CH_2]_nOR$, $n = 3-6$ and R = H or CH_3) have been shown to effectively prevent the adsorption of most proteins under a wide range of conditions.[43,44] Even mixed PEG and normal alkanethiol SAMs can effectively resist protein adsorption.[45−47] As a result, these SAMs have been used in the fabrication of protein nanoarrays and peptide-based chips to resist nonspecific protein adhesion and cell adhesion.[48]

In the experiments reported here we have used undecanethiol triethylene glycol (HSC_{11}-EG_3) as protein resistant SAMs. The theoretical height of this monolayer is 2.26 nm (assuming that the angle between SAM molecules and the surface normal is 30°: h_{SAM} = 2.21 Å (S−Au vertical distance) + 2.84 Å (distance contributed by each EO unit) × 3 + 1.25 Å (carbon−carbon distance) × 11 × cos 30° = 22.6 Å). We have confirmed this by directly measuring the SAM height via "nanoshaving"[49] experiments (data not shown), which gave h_{SAM} =2.3 nm. This result is also in agreement with previous AFM height measurements of HSC_{11}-EG_3 nanografted into C_{18} (octadecanethiol) layers.[50]

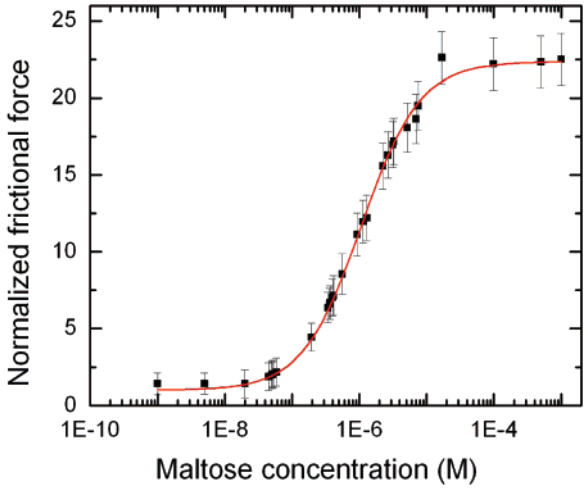

Figure 4. Normalized lateral frictional force (see text) versus maltose concentration (black squares). Error bars represent the rms values of the normalized frictional force measured for each maltose concentration. The red curve represents a fit to the data with a binding isotherm.

Figure 2a shows a typical protein patch obtained by nanografting and imaged at low force (<0.5 nN). The height of the patch above the SAM is 1 nm (Figure 2b), which gives a total height of the MBP-cys-cys protein of about 3.3 nm. This result is in good agreement with the MBP height reported in literature (the reported protein dimensions from crystallographic studies are 3.0 × 4.0 × 6.5 nm^3;[1] the height of the double cysteine linker is estimated to be approximately 0.4 nm, with a maximum height of 0.8 nm if the linker would be fully extended, which is not likely to be the case;[22] based on these data the estimated height for MBP-cys-cys is 3.4 nm).

Figure 2c shows a histogram of all height differences between the protein layers and the surrounding SAM matrix, measured for 30 patches. The average value of the height difference is 1.06 nm, giving an average measured height of the proteins of 3.36 nm. This compares very well with the height 3.4 nm estimated above. We also note that the width of the distribution of the height differences (0.92−1.2 nm) is much narrower than the analogous range for other types of proteins nanografted on Au.[21,22] Also the rate of successful experiments is larger (∼80%) in the present work than in its predecessors. We attribute this difference to the ample availability of proteins (see the protein purification section) that has allowed us to thoroughly optimize the grafting conditions.

Previous protein nanografting experiments have also reported a spontaneous exchange of proteins with the SAM C_{18} molecules.[21,22] Such an effect is minimal with the HSC_{11}-EG_3 SAM used for the present experiments. We have observed no significant spontaneous chemisorption of proteins on a time scale of 12 h. This result is consistent with the protein-resistant properties of the PEG layers previously reported in the literature. We note that, to explain this result, it is not necessary to invoke

(41) Sader, J. E. *Rev. Sci. Instrum.* **2003**, *74*, 2438−2443.
(42) Inglis, W.; Sanders, G. H. W.; Williams, P. M.; Davies, M. C.; Roberts, C. J.; Tendler, S. J. B. *Langmuir* **2001**, *17*, 7402−7405.
(43) Grosdemange, C. P.; Simon, E. S.; Prime, K. L.; Whitesides, G. M. *J. Am. Chem. Soc.* **1991**, *113*, 12−20.
(44) Deng, L.; Mrksich, M.; Whitesides, G. M. *J. Am. Chem. Soc.* **1996**, *118*, 5136−5137.
(45) Prime, K. L.; Whitesides, G. M. *J. Am. Chem. Soc.* **1993**, *115*, 10714−10721.
(46) Tan, J.; Tien, L. J.; Chen, C. S. *Langmuir* **2002**, *18*, 519−523.
(47) Roberts, C.; Chen, C. S.; Mrksich, M.; Martichonok, V.; Ingber, D. E.; Whitesides, G. M. *J. Am. Chem. Soc.* **1998**, *120*, 6548−6555.
(48) Yan, J.; Tender, L.; Hampton, M. P. D.; Lopez, G. P. *J. Phys. Chem. B* **2001**, *105*, 8905.
(49) Amro, N. A.; Xu, S.; Liu, G.-Y. *Langmuir* **2000**, *16*, 3006−3009.
(50) Hu, Y. Ph.D. thesis, Princeton University, 2005.

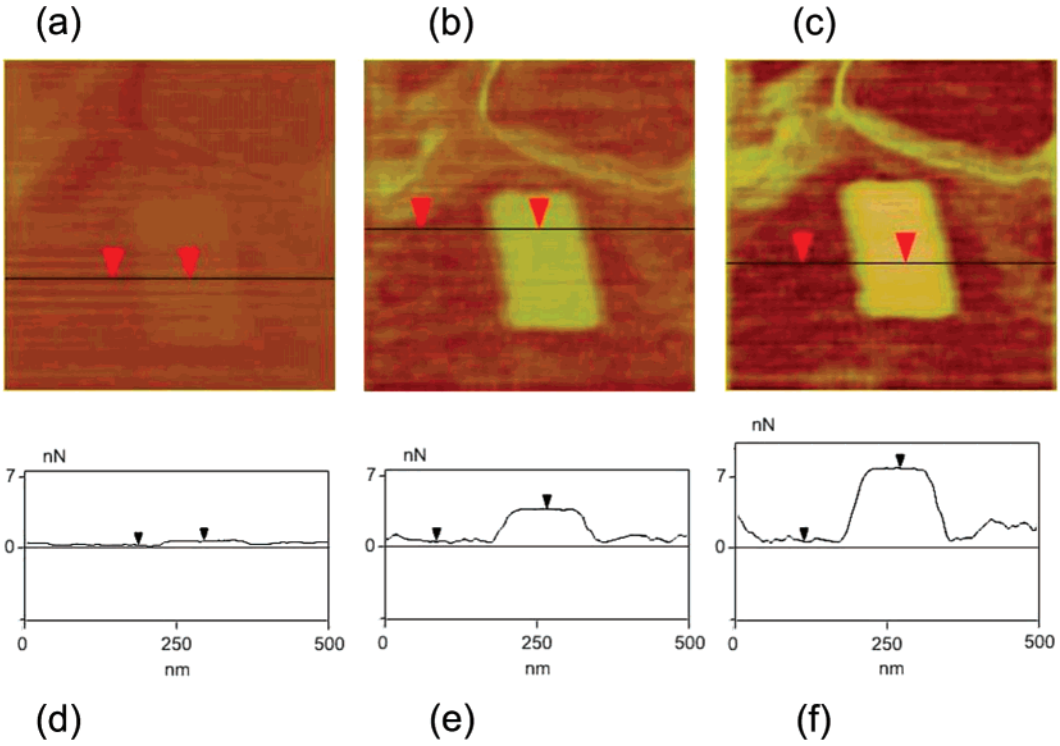

Figure 5. AFM lateral friction images for three different maltose concentrations: 1 nM (a), 1 μM (b), and 1 mM (c). (d−f) Line scans corresponding to the black lines in images (a−c).

a smaller density of defects in the PEG layers with respect to the C_{18} layers used in the previous protein grafting experiments. This is because the shorter time of temporary adsorption on the PEG surface, due to the decreased affinity of the proteins for this surface, does give a smaller chance to the proteins bound to the surface of finding the defective part of the monolayer before returning to solution.

3.2. Detection of Maltose Binding Using AFM Friction Measurements. In this section we report a new approach for the detection of ligand-binding events, based upon transducing the maltose mediated hinge bending motion of MBP into changes in frictional force between the AFM tip and the nanografted protein patch. The AFM has been widely used to study the frictional properties of molecular monolayers immobilized on Au surfaces, such as fluorinated organic films,[51,52] mixed monolayers composed of varying concentrations of the methyl- and trifluoromethyl-terminated thiols,[53] *n*- alkanethiols,[54] etc. Generally, these studies have found that SAMs which are less ordered (for example, SAMs assembled with shorter molecules) show larger friction than the SAMs with a higher degree of order between the molecules.[52,55]

Figure 3a shows the lateral friction image taken for a protein patch before introducing maltose into the buffer solution. After the protein nanopattern was made the area containing this pattern was scanned multiple times at constant, low imaging force ($F < 0.5$ nN). When the tip is above the SAM matrix, the lateral frictional force (F^0_{sub}) has an average (background) value of (0.2 ± 0.05) nN, while the same force with the tip above the protein patches is $F^0_{patch} = (0.5 \pm 0.05)$ nN (Figure 3d). Upon changing to a 0.2 μM maltose solution the values of the two frictional forces change respectively to $F^M_{sub} = (0.4 \pm 0.1)$ nN (substrate) and $F^M_{patch} = (3.5 \pm 0.1)$ nN (patch) (Figure 3b, e). Thus the relative change in the lateral frictional force upon maltose addition above the patch: $F^M_{patch}/F^0_{patch} = 7$ is about 3.5 times larger than the same change above the SAM matrix ($F^M_{sub}/F^0_{sub} = 2$). There was no significant change in the height of the patch, which remained constant at: $h = 3.4$ nm. We are led to the conclusion that the conformational change of the MBP-cys-cys protein induced by maltose binding events allows for ligand binding to be detected by AFM-friction experiments. Further, maltose binding is a reversible process: after removing the maltose by washing the patch with pure buffer for 15 min, the frictional forces (Figure 3 c, f) are restored to their initial values (Figure 3 a, d). These changes in the frictional force were reproducible upon several maltose exposure/washing cycles (data not shown).

These results are consistent with the known MBP structure and previous frictional measurements performed on organic monolayers. It is known that upon binding maltose the two MBP domains (lobes) rotate 35° and twist laterally 8° relative to each other,[1,56,57] such that overall the amino- and carboxy-termini move 7 Å closer to each other after binding. In our configuration (Figure 1) this motion takes place in a plane which is approximately parallel to the Au surface, and therefore there is no noticeable change in the protein height. Also, since the overall surface packing and order of the protein patch is not

(51) Kim, H. I.; Koini, T.; Lee, T. R.; Perry, S. S. *Langmuir* **1997**, *13*, 7192−7196.
(52) Houston, J. E.; Doelling, C. M.; Vanderlick, T. K.; Hu, Y.; Scoles, G.; Wenzl, I.; Lee, T. R. *Langmuir* **2005**, *21*, 3926−3932.
(53) Kim, H. I.; Graupe, M.; Oloba, O.; Koini, T.; Imaduddin, S.; Lee, T. R.; Perry, S. S. *Langmuir* **1999**, *15*, 3179−3185.
(54) Lio, A.; Morant, D. F.; Ogletree, D. F.; Salmeron, M. *J. Phys. Chem. B* **1997**, *101*, 4767−4773.
(55) Xiao, X.; Hu, J.; Charych, D. H.; Salmeron, M. *Langmuir* **1996**, *12*, 235−237.
(56) Sharff, A. J.; Rodseth, L. E.; Spurlino, J. C.; Quiocho, F. A. *Biochemistry* **1992**, *31*, 10657−10663.
(57) Fehr, M.; Frommer, W. B.; Lalonde, S. *Proc. Natl. Acad. Sci. U.S.A.* **2002**, *99*, 9846−9851.

likely to change, the increase in the frictional force upon binding maltose may reflect the change in the chemical nature of the locally exposed group, similar to the situation reported for alkane-thiol molecules terminated with different functional groups.[51−53] Further theoretical and experimental work is, however, needed to establish more precisely the origin of the measured changes. A strong implication of these maltose detection results is that the protein function (and therefore its tertiary structure) is maintained throughout the whole nanografting process, being largely unaffected by the addition of the double cysteine, the confinement associated with nanografting, and the interaction between the protein and the Au substrate.

3.3. AFM Friction Measurements as a Function of Maltose Concentration. Maltose-dependent changes in the frictional force were also measured by varying the maltose concentration in the buffer solution from 0 to 1 mM. The ligand concentration dependence of the frictional force is shown in Figure 4 where the variation of the *normalized* frictional force, $F_N = (F^M_{patch}/F^0_{patch}) \bullet (F^0_{sub}/F^M_{sub})$ (see section 3.2), is plotted versus the maltose concentration. Figure 5 shows an example of the measured frictional forces for a protein patch at three different maltose concentrations: low, 1 nM (Figure 5a); intermediate, 1 μM (Figure 5b); and high, 1 mM (Figure 5c).

Assuming a linear dependence between the frictional force and the fraction of bound maltose in a patch, the data in Figure 4 can be fitted with a single-site binding isotherm using the maximum response in the amount of binding (maximum frictional force) and the maltose dissociation constant k_d as free parameters.[58] The value of the dissociation constant determined from the fit to the data is $k_d = (1 \pm 0.04)$ μM which is within the range 0.2−1.2 μM reported in literature from fluorescence measurements.[32,35,36]

Moreover, we note that a relatively large (compared to the size of the detector) area of $\sim$100 μm^2 could be easily covered by small droplets of buffer containing maltose, with volumes of $\sim 10^{-6}$ mm^3. These droplets are too small to wet any macro/electrochemical detectors, but the detection could easily be accomplished using AFM-friction measurements, since the droplet area and height are larger than the patch/detector area and tip height, respectively. From Figure 4 we can see that maltose concentrations as small as 0.1 μM can be detected using this sensor. This means that the proposed friction-AFM based sensor can detect maltose at the level of tens of attograms or 10^4 maltose molecules. Therefore, the MBP-cys-cys system provides a very sensitive, surface-immobilized, protein nanobiosensor for maltose, and the AFM-friction measurements represent a new approach for detecting protein−ligand binding events and for measuring the kinetics of the binding reactions.

(58) See for example: http://www.graphpad.com/curvefit/how_to_derive.htm#example_model_3_equilibrium_binding.

4. Conclusions

We have described the nanopatterning of double-cysteine terminated Maltose Binding Protein at addressable locations onto Au substrate using an AFM based technique called nanografting. The biochemical activity of the substrate immobilized proteins was verified in situ by AFM friction measurements. The experiments demonstrate that the MBP function is not altered by the immobilization process, the spatial confinement associated with the surrounding proteins, and the protein−substrate interactions. We have also reported a new approach for the detection of ligand-binding events for this class of proteins, based upon the yet to be clarified connection between the maltose mediated hinge bending motion of MBP and the changes in frictional force between the AFM tip and the nanografted protein patch. The dependence of the frictional force upon the maltose concentration was used to extract the dissociation constant: $k_d = (1 \pm 0.04)$ μM for this system. Our data show that this friction-AFM based sensor can detect maltose at the level of tens of attograms or 10^4 maltose molecules ($\sim$100 nM maltose concentration), which is well below the sensitivity limit displayed by electrochemical based biosensors. In addition, the proposed detection method does not involve any significant modification of the protein conformation (such as for example the attachment of dye labels or quantum dots necessary for optical-based detection), and therefore the perturbation of the protein native configuration is minimal. Our findings have a few general implications for building protein-based biosensors as the immobilization process, characterization of the biological function, and detection mechanism are general, and we anticipate that it should prove to be relatively easy to apply our results to other periplasmic binding proteins such as Glucose Binding Protein, Ribose Binding Protein, Arginine Binding Protein, etc. Moreover, arrays of these proteins could be easily patterned on the same chip using nanografting.

Acknowledgment. This work was supported in part by an Institute for Complex Adaptive Matter (ICAM) postdoctoral fellowship (C.S.), in part by the National Science Foundation (NSF) funded Princeton MRSEC group grant, and in part by a grant from the U.S. Department of Energy (340-6007).

JA076157+